Metallurgical and Materials Engineering *Research paper*
Association of Metallurgical Engineers of Serbia AMES *https://doi.org/10.30544/627*

DENSITY FUNCTIONAL PREDICTION OF THE STRUCTURAL, ELASTIC, ELECTRONIC, AND THERMODYNAMIC PROPERTIES OF THE CUBIC AND HEXAGONAL (*c*, *h*)-Fe_2Hf

M. Hamici[1] , T. Chihi[2], M.A Ghebouli[2], M. Fatmi[2,], B. Ghebouli[3], S. I. Ahmed [4]*

[1] Dosage Analysis and Characterization Laboratory (DAC), University Farhet Abbas of Setif 1, 19000, Algeria
[2] Research Unit on Emerging Materials (RUEM), University Farhet Abbas of Setif 1, 19000, Algeria
[3] Laboratory of Studies Surfaces and Interfaces of Solids Materials, Department of Physics, Faculty of Sciences, University Ferhat Abbas of Setif 1, 19000, Algeria
[4] Department of Physics, College of Science, Taif University, P.O. Box 11099, Taif 21944, Saudi Arabia

Received 23.03.2021
Accepted 09.06.2021

Abstract

Using density functional theory (DFT), the structural, elastic, electronic, and thermodynamic properties of Fe_2Hf in the cubic and hexagonal solid phases with *Fd-3m* and *P63/mmc* are reported with generalized gradient approximations (GGA). To achieve energy convergence, we report the k-point mesh density and plane-wave energy cut-offs. The calculated equilibrium parameters are in good agreement with the available theoretical data. A complete elastic tensor and crystal anisotropies of the ultra-incompressible Fe_2Hf are determined in the wide pressure range. Finally, by using the quasi-harmonic Debye Model, the isothermal and adiabatic bulk modulus and heat capacity of Fe_2Hf are also successfully obtained in the present work. By the elastic stability criteria, it is predicted that *Fd-3m* and *P63/mmc* structures of Fe_2Hf are stable in the pressure range studied, respectively.

Keywords: elastic stability; thermodynamic properties; Fe_2Hf compound.

[*]Corresponding author: M. Fatmi, *fatmimessaoud@yahoo.fr*

Introduction

Up to now, Fe_2Hf structures are not still synthesized in crystalline form. We have proposed two structures of cubic and hexagonal type structures. Elastic constants under pressure play an important role in determining the strength and hardness of materials. They are very important to determine the response of the crystal to external forces, as characterized by the bulk and shear modulus. The elastic properties of two cubic and hexagonal structures are also explored. However, to our knowledge, no works have reported on the elastic, structural, and thermodynamic properties of hexagonal structures of Fe_2Hf under pressures. *Koki Ikeda et al.* [1] studied the crystal structures and magnetic properties of the stoichiometric Laves phase in the iron hafnium system by X-ray powder techniques and magnetization measurements. They concluded that the hexagonal $MgZn_2$-type Fe_2Hf compound occurs above 1673 K, and the cubic $MgCu_2$-type exists below 1273 K.

S. Kobayashi *et al*. [2-3] have observed periodically arrayed rows of fine Fe_2Hf Laves phase particles formed in 9 % chromium ferritic matrix and propose a new strategy for controlling precipitation of Laves phase for further improving the long term creep resistance of ferritic steels. *J. Belosevic-Cavor et al*. [4] studied the magnetic properties, Mossbauer Effect and first principle calculations of laves phase Fe_2Hf with C14 type structure. Hexagonal lattice was found for Fe_2Hf by Masao Takeyama [5] with space group *P63/mmc* (N°194). Fe_2Hf has a C15 cubic structure of $MgCu_2$ type which exists in a narrow composition range around the stoichiometry. Additionally, it crystallizes in $MgZn_2$ (C14) hexagonal structure type, and the hexagonal phase appears in addition to the predominant cubic phase. Our primary aim was, therefore, to present the results of a theoretical investigation of the structural and thermodynamic of (*c*, *h*)-Fe_2Hf. The *c*-Fe_2Hf (*h*-Fe_2Hf) structures are cubic (hexagonal) with space group 227, *Fd-3m*with Cu_2Mg-type (194, *P63/mmc* with Zn_2Mg-type), non-equivalent atoms are Fe in (0.625, 0.625, 0.625); and Hf in (0, 0, 0); (a=6.882Å) (Fe_1 in (0, 0, 0); Fe_2 in (0.8, 0.6, 0.25) and Hf in (1/3, 2/3, 0.06); (a=b= 4.968Å, c=8.098Å)) with one (two) for *c*-Fe_2Hf (*h*-Fe_2Hf) formula units per unit cell.

Computational details

CASTEP was the first-principles plane-wave pseudo-potential method based on the density functional theory, the crystal wave functions launched by Plane Wavelet Group using periodic boundary conditions, in which the exchange-correlation potential adopted GGA. Without taking into account the spin polarized, we must first investigate and examine the convergence of calculated total energies with respect to the plane wave cut-off E_{cut} in the cubic and hexagonal solid phases of the two molecular systems to be 380eV (385eV) for *c*-Fe_2Hf (*h*-Fe_2Hf) Fig.1 (a) and (b) respectively. The number of points can be arbitrarily increased to increase the precision of calculations but this increases the computational cost.

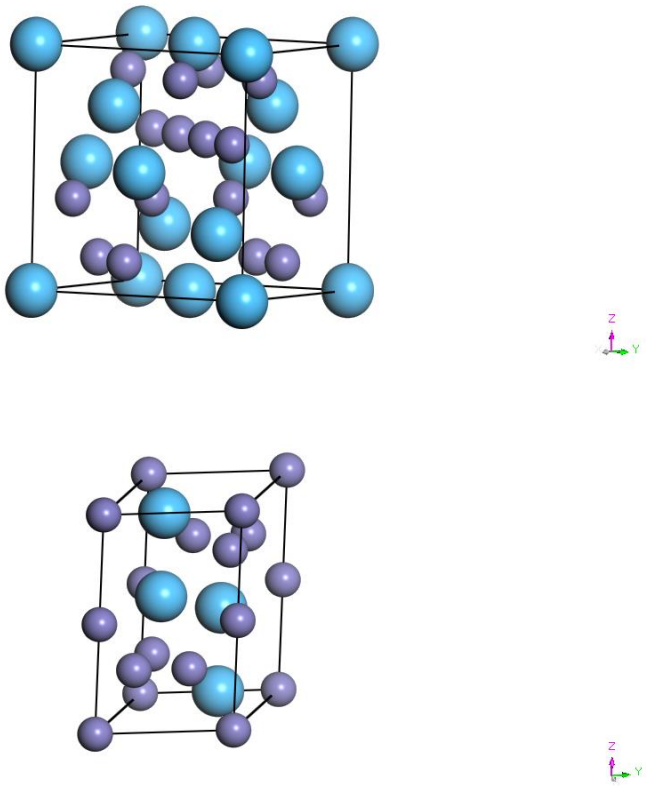

Fig. 1. Unit-cell of Fe_2Hf cubic and hexagonal crystal, the large and small balls represent Hf and Fe atoms, respectively.

Structural properties

In this work, we focus on structural, elastic, electronic, and thermodynamic properties of Fe_2Hf with cubic (hexagonal) structures under pressures up to 10GPa (15GPa) by first-principles calculations. The elastic properties of two cubic and hexagonal structures of Fe_2H funder pressure are investigated for the first time, from which the mechanical stability is also determined. In order to further investigate Fe_2Hf the thermodynamic properties, such as the heat capacity, thermal expansion, Debye temperature, and so on, are obtained by Debye model. However, it is difficult to study experimentally because of the extremely small sizes and time scales at which the functional properties appear. Theoretical modeling, on the other hand, offers a way to overcome these difficulties through "virtual experiments" that can enable us to quickly, efficiently, and affordably explore phase space. Density functional theory (DFT) is one of the most successful quantum mechanical theory based tools to characterize properties of materials, and it is widely used in quantum computation in condensed matter physics [6-8]. DFT is a general-purpose computational method and can be applied to most

systems. Although density functional theory is more accurate and exact in theory, its implementation requires several approximations such as the choice of basis-set, exchange-correlation [9-11] functional, mesh-size for Brillouin zone [12-14] for plane-wave basis.

The plane wave cut-off is the parameter that controls such truncation, so the more include plane waves; the better the wave function is modeled. The k-point mesh controls the BZ integration, can play a huge role in the quality of the results, and heavily depends on the number of these points on the mesh-grid, especially for metals. The plane wave basis set in the DFT wave function is expanded in terms of a: due to its periodicity and ease of use. Each function $u_i.k(r)$ is expressed as a Fourier series whose basis states are plane waves whose wave vector is a reciprocal lattice vector G (which are defined by $e^{iG \cdot R} = 1$).

The DFT wave function is expanded in terms of a plane wave basis set:

$$\psi(r) = \sum_G C_G e^{i(G+K)r} \quad 1$$

where, G is the reciprocal wave vector, k is k-point vector, C_G are the expansion coefficients. There is an infinite number of allowed G, but the coefficient C_G becomes smaller and smaller as G^2 becomes larger and larger. The cut-off energy E_{cut} is defined [15] as:

$$E_{cut} = \frac{\hbar^2}{2m}|G_{cut}|^2 \quad 2$$

$$|G + K| < E_{cut} \quad 3$$

Any standard DFT code such as CASTEP uses the total energy convergence rather than energy per atom during an SCF procedure. Fig.1; represents total energy as a function of the number of k-points. The convergence has been achieved in the k-points sampling of 1x1x1 for total energy convergence tolerance ($1.0\ 10^{-6}$eV/atom).

The rest of this paper is structured as follows. The computational method is described in section 2. The results and some discussions of structural, elastic, and thermodynamic properties of Fe_2Hf under pressure are presented and compared with available experimental and theoretical data in section 3. Conclusions derived from our calculations are drawn in section 4. The large and small balls represent Fe and Hf atoms, respectively, as shown in Fig. 2. Secondly, we examine the convergence of the calculated number of points of our computed compounds that are 6x6x6 of *c*-Fe_2Hf and *h*-Fe_2Hf, Fig. 3. In Fig. 4, we show the plot of energy versus volume of Fe_2Hf in cubic (a) and hexagonal (b) structures. The density functional calculations on the structural, elastic, and thermodynamic properties of cubic and hexagonal structures of Fe_2Hf were performed using the CASTEP code [16,17]. Both lattices were optimized to get the equilibrium structure for cubic and hexagonal structures of Fe_2Hf. The exchange-correlation function was treated by both the generalized gradient approximation (GGA-PBE) [18]. Also, the pseudo potentials constructed using the *ab initio* ultra-soft scheme to describe the valence electron interaction with the atomic core, in which the Fe ($3d^6 4s^2$) and Hf ($4f^{14} 5d^2 6s^2$) orbital are treated as valence electrons. The Brillouin zone sampling was carried out using the 6x6x6for cubic and hexagonal structures of Fe_2Hf set of Monkhorst-Pack mesh [13]. The structures were optimized using the Broyden-

Fletcher-Goldfarb-Shenno (BFGS) minimization technique in order to achieve the most stable structure in their local area. Self-consistent convergence condition setting: the total energy was less than 0.2 eV/atom, the force in each atom was less than 0.05eV/Å, the offset tolerance was less than 0.0002 A, and the Stress bias was less than 0.1GPa. For comparison and as shown in Table 1, it should be noted that the calculated total energies of cubic and hexagonal (*c- h*)- Fe_2Hf structures are with a negative value corresponding to an exothermic reaction. The total energies show that the hexagonal structures are more stable than cubic ones.

Table 1. The calculated lattice constant (Å), volumes (Å^3), bulk modulus, elastic constants, shear modulus, Young's modulus, B/G ratio, density, sound velocities, and Debye temperature for (c- h)- Fe_2Hf structures.

	Cubic structure	Hexagonal structure
Cuttofenegy (eV)	380	385
KxKxK	6x6x6	6x6x6
Total energy (eV)	-4280.10	-8560.42
a(Å)	4.883	4.858 (4.968)
b(Å)	4.883	4.858(4.968)
c(Å)	4.883	8.042(8.098)
Volume (Å^3)	82.340	164.456
Z	2	1
B(GPa)	218.90	222.496
C_{11}	316.256	358.613
C_{12}	170.230	180.066
C_{44}	96.075	91.652
C_{33}	-	347.149
C_{13}	-	146.081
C_s	86.075	93.721
ρ	11.0766	11.7201
v_l(m/s)	5488.5230	5447,6170
v_t(m/s)	2787.6312	2827,834
v_m(m/s)	3123.573	3164,9355
Θ_D (K)	378	394
Y	230.119	246.595
ν	0.32479	0.31557

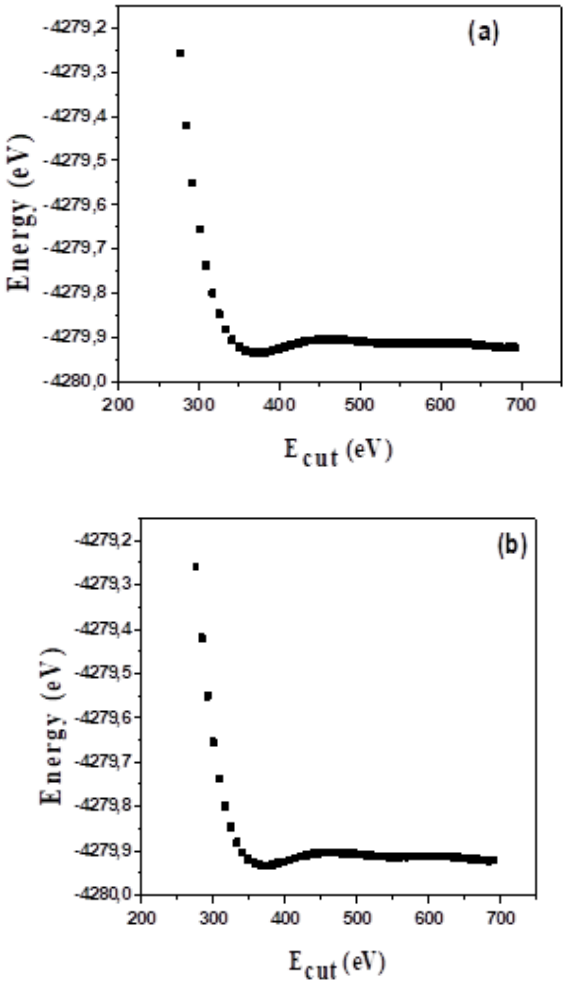

Fig. 2. Energy versus E_{cut} in cubic (a) and hexagonal (b) structure.

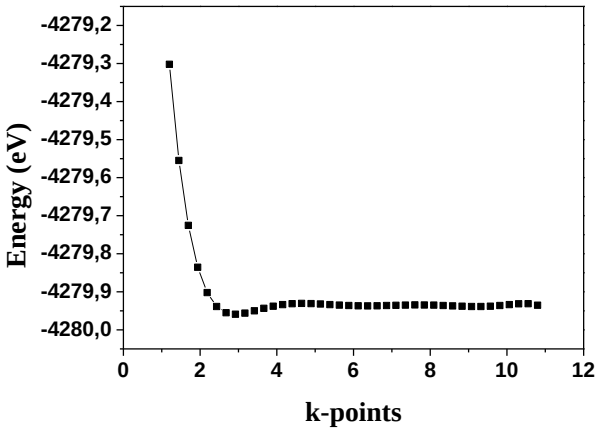

Fig. 3. Energy versus number of k points of our computed compounds.

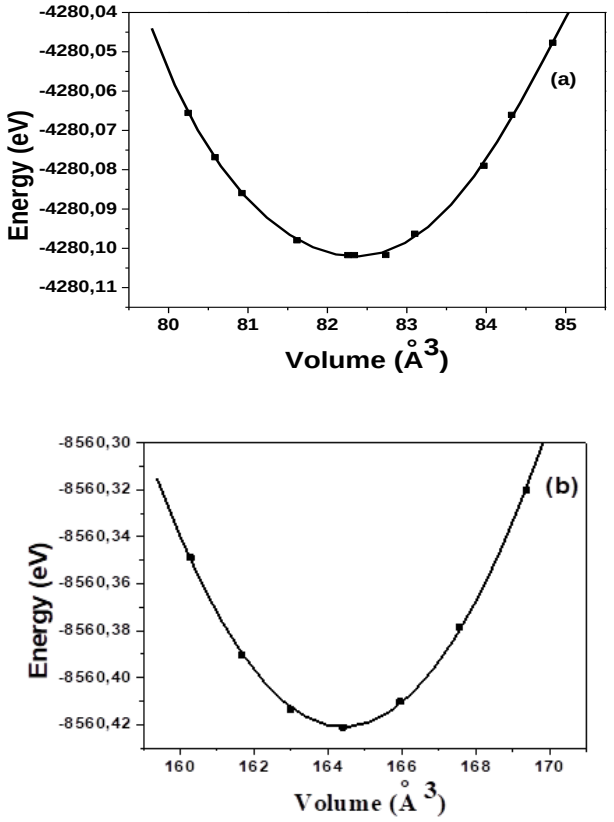

Fig. 4. Energy versus volume for Fe_2Hf in cubic (a) and hexagonal (b) structure.

Elastic constants

By means of a Taylor series expansion of the total energy, E (V, δ), the elastic constants are defined for the system compared to a small deformation δ of the lattice unit cell volume V. The energy of system constraint is expressed as follows [19]:

$$E(V,\delta) = E(V_0,0) + V_0[\sum_i \tau_i \xi_i \delta_i + \frac{1}{2}\sum_{ij} C_{ij}\delta_i \xi_i \delta_j] \quad 4$$

Where $E(V_0, 0)$ is the energy of the unstrained system with equilibrium volume V_0, τ_i is an element in the stress tensor, and ξ_i is a factor to take care of the Voigt index. Between 21 and 2 independent elastic constants, corresponds respectively to asymmetric material and isotropic material, the number of independent elastic constants is 3 for cubic and 5 for hexagonal crystals. These three independent elastic constants are usually referred to as C_{11}, C_{44}, and C_{12} for cubic and C_{11}, C_{33}, C_{44}, C_{12}, and C_{13} for hexagonal crystals. A theoretical treatment of the elasticity of hexagonal systems is thus considerably more involved than for cubic structure, which has three independent elastic constants. The elastic constants of solids provide a link between mechanical and dynamical behaviours of crystals and give important information concerning the nature of forces operating in solids. In particular, they provide information on the stability and stiffness of materials. It is well known that first-order and second-order derivatives of the potential give forces and elastic constants. Therefore, it is an important issue to check the accuracy of the calculations for forces and elastic constants. Let us recall here that the pressure effect upon elastic constants is essential, at least for understanding interatomic interactions, mechanical stability, and phase transition mechanism. The corresponding bulk moduli are determined as a function of pressure up to 50 GPa for cubic and hexagonal Fe_2Hf structures. Let us notice that all elastic constants, as well as both bulk moduli, linearly increase when pressure is enhanced Fig. 5. The bulk modulus was obtained from a calculation of the three cubic elastic constants C_{11}, $C_{12}$and C_{44} using the expression:

$$B = (C_{11} + 2C_{12})/3 \quad 5$$

The calculated bulk value with the second method is agreeable with the bulk modulus, which is deducted from the first method. For Fe_2Hfin, a cubic crystal, the generalized elastic stability criteria in terms of elastic constants [20]:

$$(C_{11} + 2C_{12})/3 > 0 \qquad C_{44} > 0 \quad 6$$

$$(C_{11} - C_{12})/2 > 0 \quad 7$$

For Fe_2Hf in a hexagonal crystal, let us recall that the generalized elastic stability criteria [21] are:

$$C_{11} > 0, C_{33} > 0,\ C_{44} > 0,\ C_{66} > 0\ , C_{11} - C_{12} > 0, C_{11} + C_{33} + C_{12} > 0,$$

$$(C_{11} + C_{12})C_{33} - 2C_{13}^2 > 0 \quad 8$$

The fact that the elastic constants of (Fe_2Hf) in the cubic [hexagonal] crystal do not obey all the above criteria indicates that it is an elastically unstable [stable] structure. For $Fe_2Hf$with hexagonal structure, the shear anisotropy factor $A(C_{ij})$, defined as $A=4C_{44}/(C_{11}+C_{33}-2C_{13})$ = 0.88 for the {100} shear planes between the < 011> and< 010> directions, [22] as well as the ratio between linear compressibility coefficients for hexagonal crystals, i.e. $k_c/k_a= (C_{11}+C_{12}-2C_{13})/(C_{33}-C_{13})$ = 1.22.

For hexagonal structures, bulk modulus B and shear modulus G are obtained as follows:

$$B = \frac{2}{9}\left(C_{11} + C_{12} + 2C_{13} + \frac{1}{2}C_{33}\right) \quad 9$$

$$G = \left\{C_{44}[C_{44}(C_{11} - C_{12})/2]^{1/2}\right\}^{1/2} \quad 10$$

In addition, Young's modulus E can be obtained according to *Cline et al.* [23]:

$$E = \frac{[C_{33}(C_{11}+C_{12})-2C_{13}^2](C_{11}-C_{12})}{C_{11}C_{33}-C_{13}^2} \quad 11$$

Whereas anisotropy value A and Poisson ratio are expressed as:

$$A = \frac{2C_{44}}{C_{11}-C_{12}} \quad 12$$

$$\nu = \frac{C_{12}C_{33}-C_{13}^2}{C_{11}C_{33}-C_{13}^2} \quad 13$$

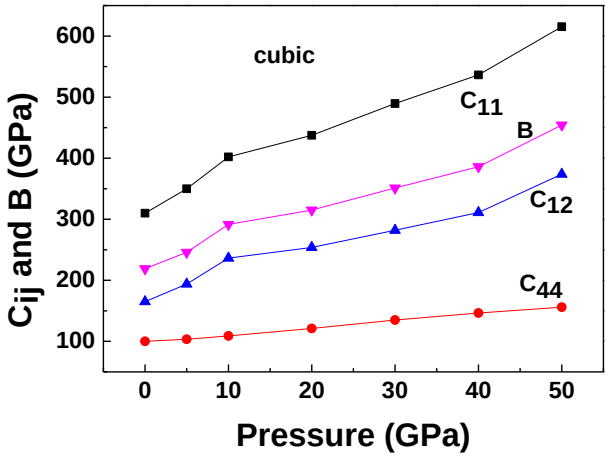

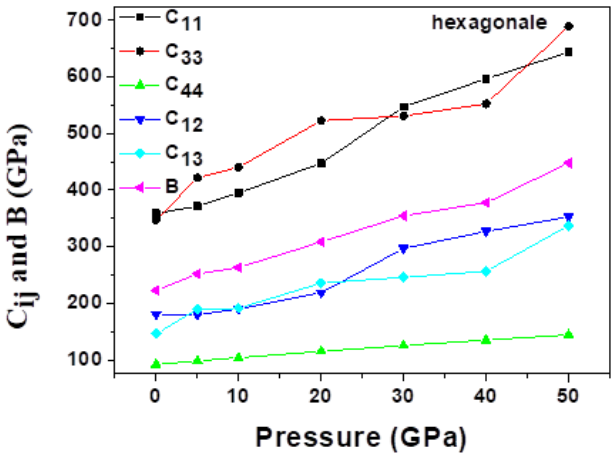

Fig. 5. The elastic constants of the cubic and hexagonal structures of Fe_2Hf compound under pressure up to 50 GPa at 0 K.

We can conclude that the bulk modulus is 219 GPa for cubic Fe_2Hf and 222 GPa for hexagonal one. All values are exceptionally high, exceeding or matching other hard materials, including boron carbide (B_4C, 200 GPa), silicon carbide (SiC, 248 GPa), sapphire (Al_2O_3, 252 GPa), and cubic boron nitride (*c*-BN, 367 GPa) [24]. Pugh [25] proposed the B/G ratio to represent a measure of a "machine able behavior". A high B/G (2.44 for hexagonal Fe_2Hf type structure) value is then associated with ductility and a low value with brittleness. The critical value which separates ductile and brittle behaviors is at about 1.75. For example, diamond has a B/G of 0.80 [26], while aluminum, cobalt, rhodium, and iridium present B/G ratios of 2.74, 2.43, 1.77, and 1.74, respectively [25]. The B/G calculated ratios for the hexagonal structure ofFe_2Hfcompound, we obtain is of 2.44. The fact of Fe_2Hf compounds is ductile compound. Additionally, the mechanical stability of the hexagonal structure at 0 GPa can be predicted from the elastic constants data ($C_{11} - C_{12} > 0$). To be complete, the elastic constants of pure Fe_2Hf in cubic and hexagonal structures are listed in Table 1. The Debye temperature may be estimated from the average sound velocity V_m [26].

$$\Theta = \frac{h}{k}\left[\frac{3n}{4\pi}\left(\frac{N_A\rho}{M}\right)\right]^{1/3} V_m \qquad 14$$

where h is Planck's constants, k is Boltzman's constant, N_A is Avogadro's number, n is the number of atoms per formula unit, M is the molecular mass per formula unit, ρ is the density, and V_m is obtained from [27].

$$V_m = \left[\frac{1}{3}\left(\frac{2}{V_s^3} + \frac{1}{V_l^3}\right)\right]^{-1/3} \qquad 15$$

where V_s and V_l are the shear and longitudinal sound velocities, respectively.

The arithmetic average of the Voigt and the Reuss bounds is called the Voigt–Reuss–Hill (VRH) average and is commonly used to estimate elastic moduli of polycrystals. The VRH averages for shear modulus (G) and bulk modulus (B) are;

$$G = \frac{1}{2}\left(G_R + G_V\right), \quad B = \frac{1}{2}\left(B_R + B_V\right) \qquad 16$$

The polycrystalline moduli are the arithmetic mean values of the Voigt and Reuss moduli [28]:

$$G_H = \frac{1}{2}(G_R + G_V), \quad B_H = \frac{1}{2}(B_R + B_V) \qquad 17$$

Therefore, the probable values of the average shear and longitudinal sound velocities can be calculated from Navier's equation [29]:

$$V_S = \sqrt{\frac{G_H}{\rho}}, \quad V_L = \sqrt{\frac{\left(B_H + \frac{4}{3}G_H\right)}{\rho}} \qquad 18$$

The longitudinal, transverse and average sound velocities and Debye temperature of cubic and hexagonal of Fe_2Hfin cubic and hexagonal structures have been calculated and listed in the Table 1.

At zero pressure and zero temperature, we obtain, as shown in Table 1, we have calculated the sound velocities and Debye temperature for the Fe_2Hf compounds from our elastic constants. Our calculated sound velocities and Debye temperature are comparable to the experimental values.

Electronic structure

In this part, the electronic properties of Fe_2Hf in a cubic and hexagonal structure are discussed. Fig. 6 shows the total density of states (DOS) for our compound in cubic and hexagonal structures at equilibrium lattice constants. We show here only the vicinity of the Fermi energy level. Fe_2Hf in cubic [hexagonal] structure have similar DOS profiles in the whole energy region except for some differences. On the other hand, near the Fermi level, the DOS mainly originates from the M-*d* bands M (Fe_2Hf) in cubic and hexagonal structure, this suggests that our compounds are all conductive, and the *d* bands of the transition metal play the dominant role in electrical transport, this phenomenon is very pronounced especially in the hexagonal structure. The DOS at the Fermi level $n(E_F)$ is calculated to be 10.69 states/eV unit cell for cubic Fe_2Hf and 20.11 eV for hexagonal of Fe_2Hf in cubic and hexagonal structure indicating the metallic material. Generally speaking, the smaller $n(E_F)$ is, the more stable the compound is. So in agreement with the results obtained from the total energy minimum.

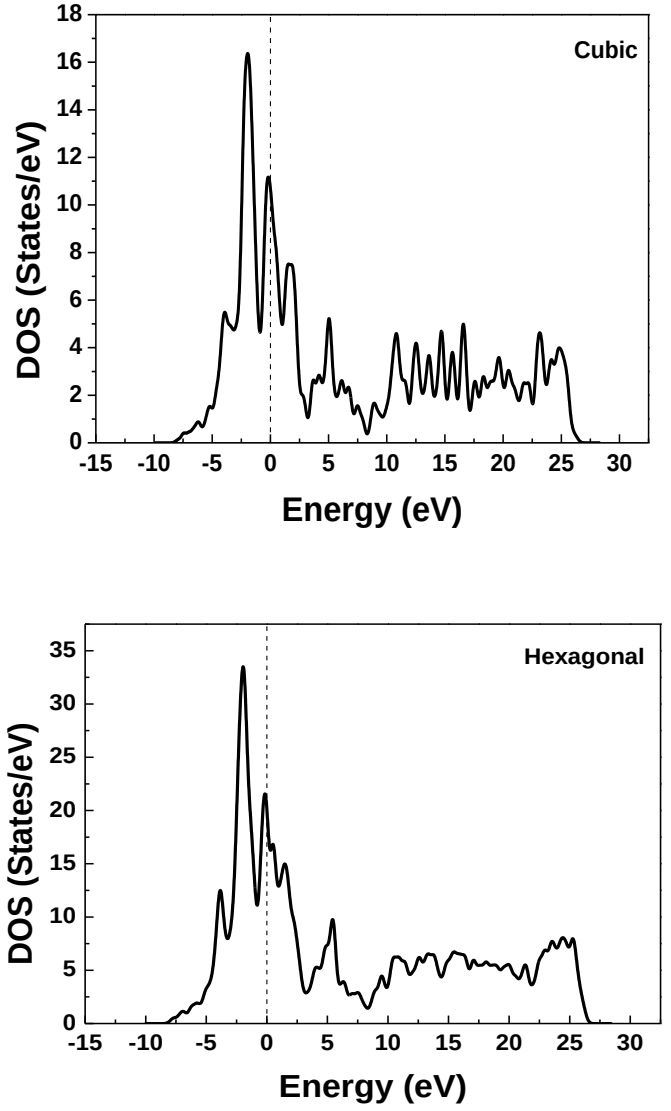

Fig. 6. The total electronic density of state for Fe_2Hf in cubic and hexagonal structures.

Thermodynamic properties

A study of the effects of chemistry and crystal structure must be performed for motors with operating temperatures in the region of 2000 °C that will require materials that can withstand. Intermetallic compounds with high melting temperatures are candidates for these applications. Thermodynamics is one of the great theories on which the current understanding of the material is based; thermodynamics is mainly based on temperature and entropy, which is the degree of disorganization of the material. Physical properties under pressures and temperatures have important meanings to accelerate the understanding and synthesis of (*c*, *h*)- Fe_2Hf structures. The investigation of the thermal capacity of crystals is an interesting subject in solid state physics because it enters many applications and provides essential information on its vibratory properties. According to the standard theory of elastic continuum, two limiting cases are correctly predicted. At sufficiently low temperatures, the thermal capacity C_V is proportional to T^3. At high temperatures, C_V tends to the limit Petit and Dulong. Applying the quasi-harmonic Debye model to the (*c*, *h*)- Fe_2Hf structures, we calculated the thermal capacity of the C_V, network and the Debye temperature θ at different temperatures. Now we investigate the dependences of bulk modulus B on temperature T and pressure P. B is plotted in Fig. 7.

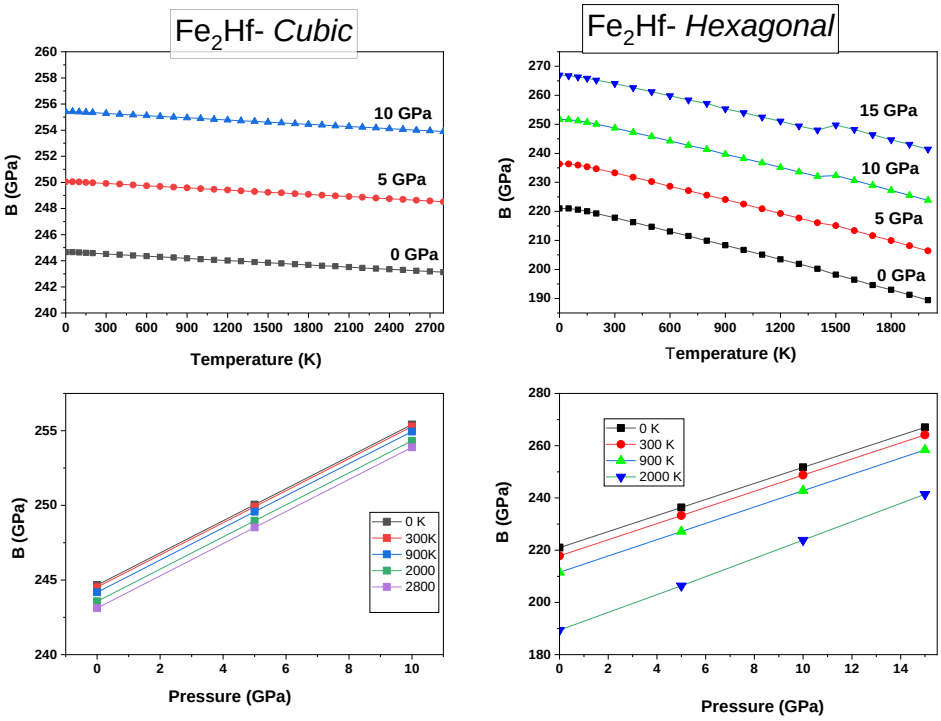

Fig. 7. Variation of bulk modulus with temperature T at various pressures for c- Fe_2Hf and h- Fe_2Hf (upper panel) respectively. Effect of pressure on bulk modulus at different temperatures for c- Fe_2Hf and h- Fe_2Hf (lower panel), respectively.

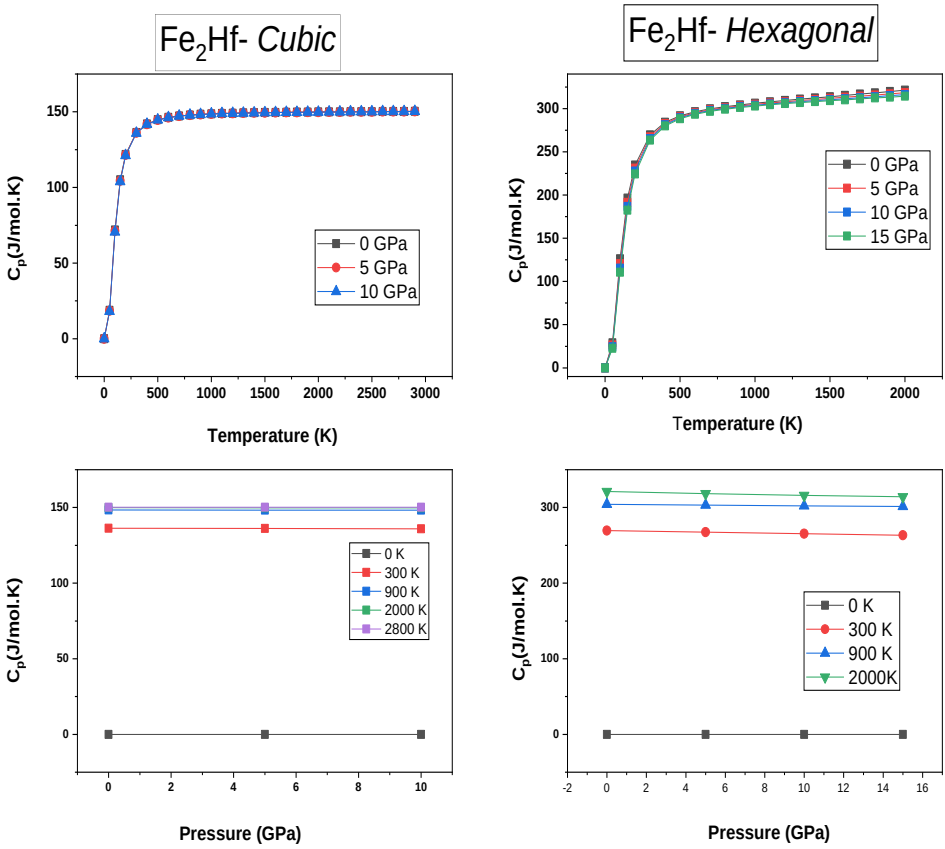

Fig. 8. Variation of constant pressure heat capacity C_P with temperature T at various pressures for c- Fe_2Hf and h- Fe_2Hf (upper panel) respectively. Effect of pressure on constant pressure heat capacity C_P at different temperatures for c- Fe_2Hf and h- Fe_2Hf (lower panel), respectively.

The bulk modulus *B* decreases with increasing temperature in a quasi-linear manner for both *c*- Fe_2Hf and *h*- Fe_2Hf structures. The calculated bulk modulus B_0 at (T = 0K) is 244.5GPa for *c*- Fe_2Hf and222GPa for *h*- Fe_2Hf structures. We can see that the bulk modulus decreases [increases] with temperature (upper panel) [pressure] [lower panel] at a given pressure [temperature] thus for both *c*- Fe_2Hf (slowly decreases) and *h*- Fe_2Hf structures. The resulting Debye temperature Θ versus temperature [Pressure] (upper panel) [lower panel] for *c*- Fe_2Hf and *h*- Fe_2Hf structures shows in Fig. 9. From the quasi-harmonic Debye model, we obtained the Debye temperature Θ = 415.5 K and 458 K at P=0 GPa and T=0 K for respectively *c*- Fe_2Hf and *h*- Fe_2Hf structures. The heat capacity C_P and C_V, represents the heat absorbed by the crystal at constant pressure or constant volume necessary to raise the temperature of one mole of a pure substance by one-degree K generated by this transformation. The heat capacity of a crystal is given by a relation deduced from the vibratory motions of the crystal lattice it is also mandatory for many applications. For solids and liquids, the variation of the PV product

with the temperature is negligible. Consequently, in the condensed phase, the volume and constant pressure heat capacities have similar values $C_P \sim C_V$ for both *c*- Fe_2Hf and *h*- Fe_2Hf structures. The calculated specific heats C_P [C_V] versus temperature at different pressures for fixed pressures [volumes] (upper panel) for (*c*-*h*)-Fe_2Hf, respectively, and C_P [C_V] versus pressures at different temperatures (lower panel) are shown in Figs. 8-10. From this figure, one can see the sharp increase of C_P and C_V in the temperature range from 0up to ~500 K, and at high temperature, the C_P and C_V tend to a constant value (300 $J \cdot mol^{-1}K^{-1}$) [150 $J \cdot mol^{-1}K^{-1}$] for (*c*- *h*)- Fe_2Hf the so-called Dulong-Petit limit of $3nk_B$ value [30]. We can conclude that the volume heat capacity in 300°K is in the range of 120- 150 $J \cdot mol^{-1}K^{-1}$ for *c*- Fe_2Hf and 250-300 $J \cdot mol^{-1}K^{-1}$for *h*- Fe_2Hf. All values in this range are exceptionally high, exceeding or matching other hard materials, including silicon oxide (SiO_2, 71.5 $J \cdot mol^{-1}K^{-1}$), sapphire (Al_2O_3, 120.5 $J \cdot mol^{-1}K^{-1}$), and (Cr_2O_3, 125.1 $J \cdot mol^{-1}K^{-1}$) and approaching that of diamond (B_0 = 442 GPa).

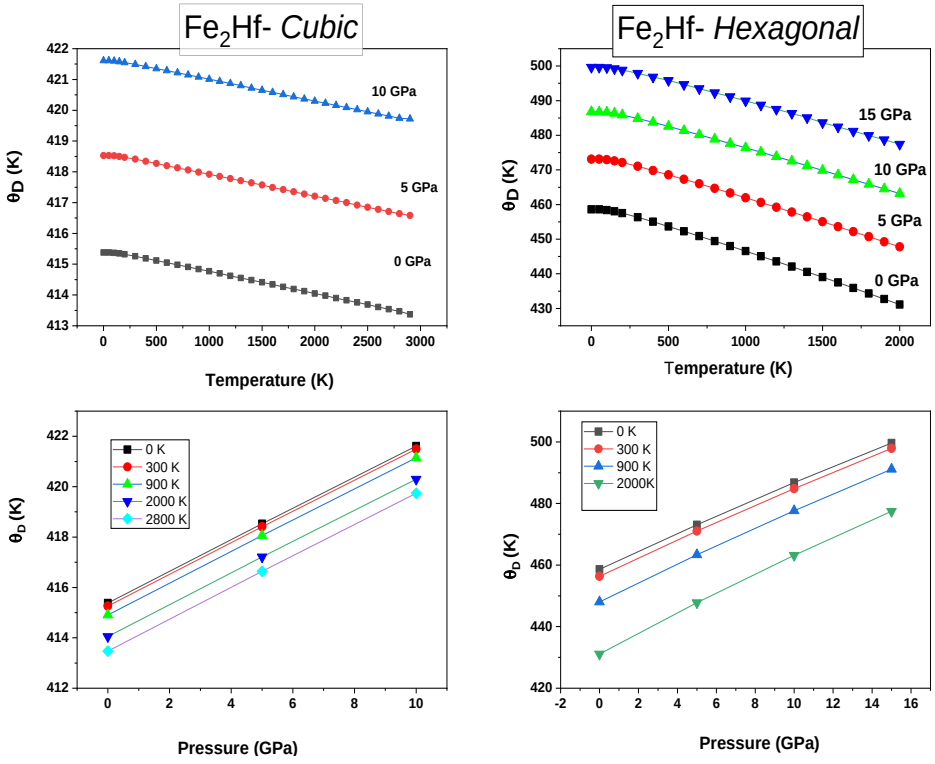

Fig. 9. Variation of Debye temperature with temperature T at various pressures for c-Fe_2Hf and h- Fe_2Hf (upper panel) respectively. Effect of pressure on Debye temperature at different temperatures for c- Fe_2Hf and h- Fe_2Hf (lower panel), respectively.

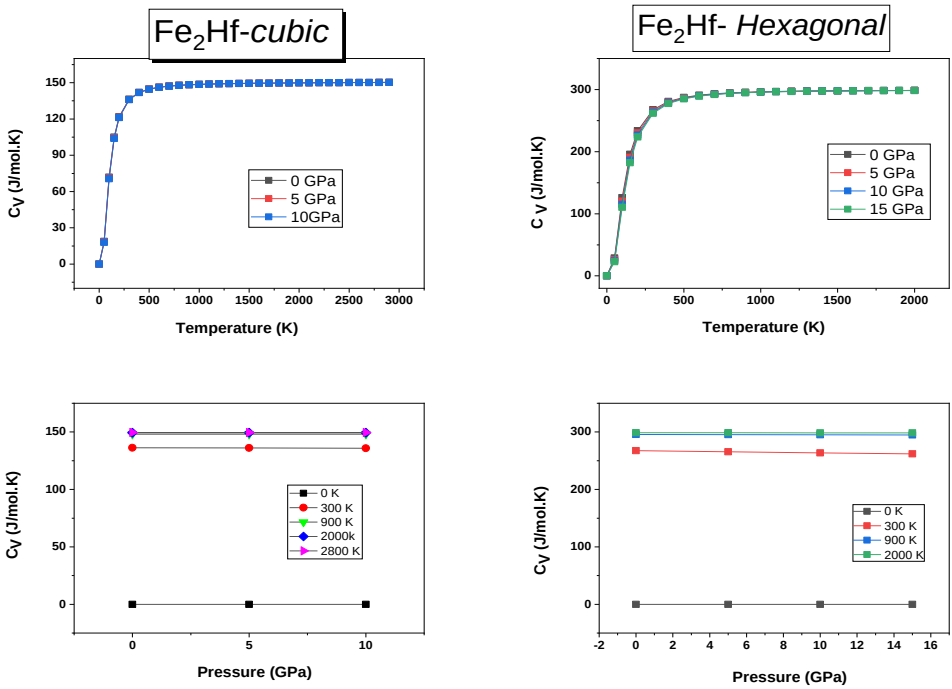

Fig. 10. Variation of constant volume heat capacity C_V with temperature T at various pressures for c- Fe_2Hf and h- Fe_2Hf (upper panel) respectively. Effect of pressure on constant volume heat capacity C_V at different temperatures for c- Fe_2Hf and h- Fe_2Hf (lower panel), respectively.

The volume expansion coefficient α_of (c, h)-Fe_2Hf structures as a function of temperature (upper panel) and pressure (lower panel) is plotted in Fig. 11. At zero pressure and 300 K, $\alpha = 0.41242 \times 10^{-5}$ K^{-1} for c-Fe_2Hf and 0.42234×10^{-5} K−1 for h-Fe_2Hf. It is shown that, for a given pressure [temperature], α increases [constant] with temperature [pressure], especially at 0 pressure, and gradually tends to a linear increase at high temperature, for c- Fe_2Hf and slightly different for h- Fe_2Hf structures. We show in Fig. 12, the entropy function of the temperature at different pressures and of the pressure at different temperatures of the two types of c- Fe_2Hf and h- Fe_2Hf structures of the compound. We show that the entropy increase parabolically with increasing temperature. We notice that these curves have the same shape except the existence of a slight offset at high temperatures especially for the case of the hexagonal type (upper panel). In the lower panel we show the variation of the entropy function S, as a function of the pressures and at different temperatures for the two types of c- Fe_2Hf and h- Fe_2Hf structures, we notice that these curves are similar and that the entropy function S is significant in the case of the hexagonal type.

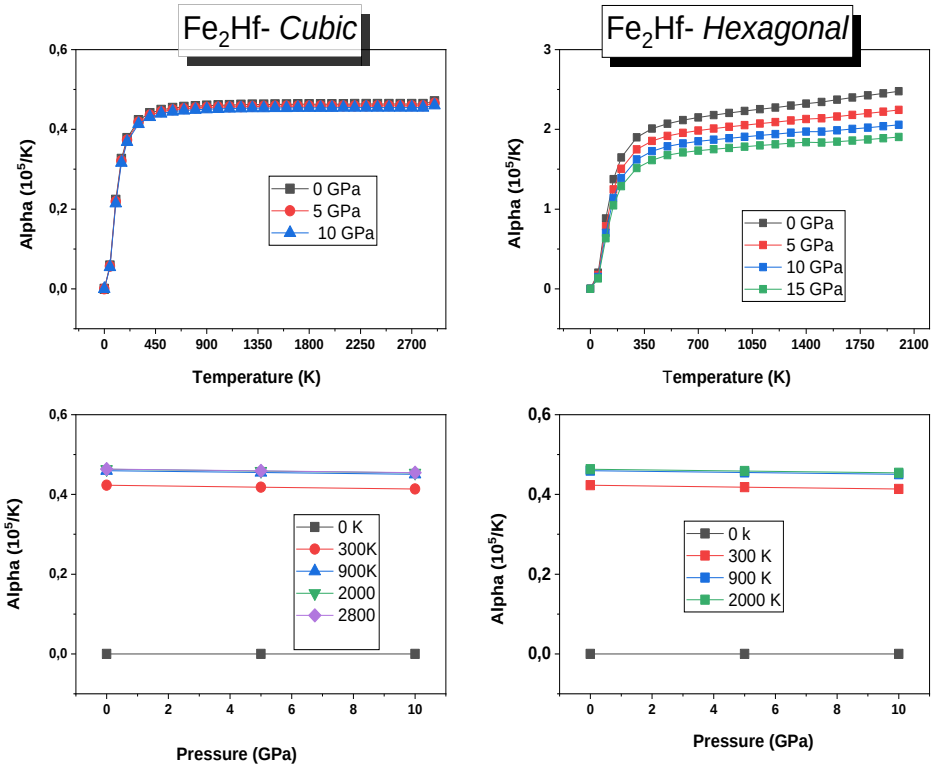

Fig. 11. Variation of volume expansion coefficient α with temperature T at various pressures for c- Fe_2Hf and h- Fe_2Hf (upper panel) respectively. Effect of pressure on volume expansion coefficient α at different temperatures for c- Fe_2Hf and h- Fe_2Hf (lower panel), respectively.

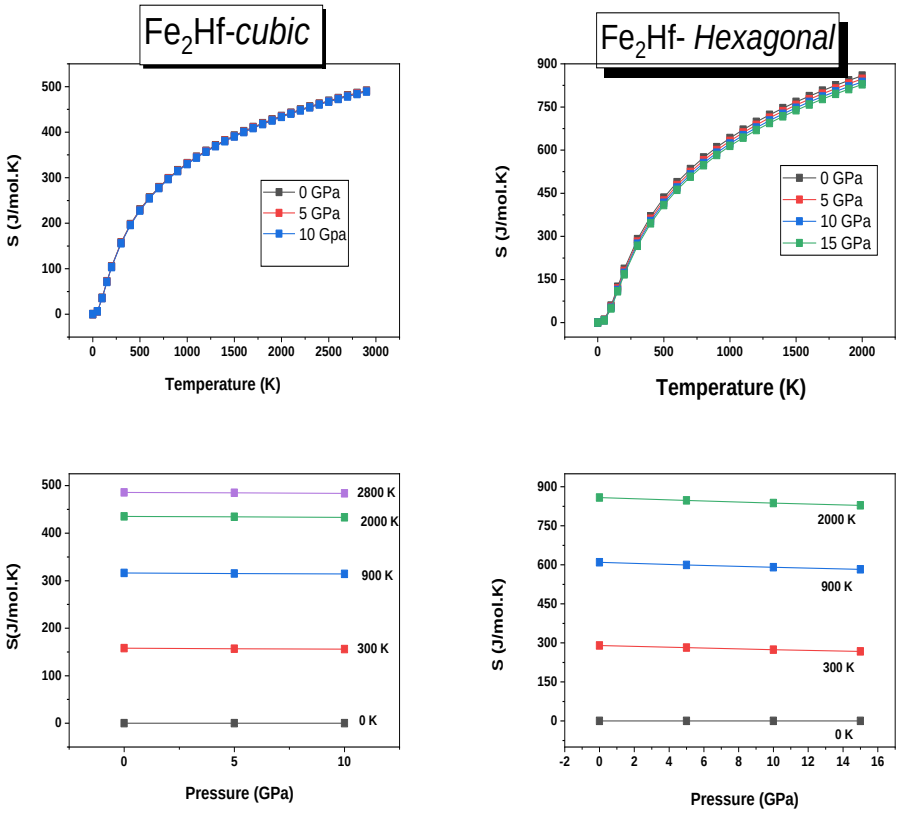

Fig. 12. Variation of entropy S with temperature T at various pressures for c- Fe_2Hf and h- Fe_2Hf (upper panel) respectively. Effect of pressure on entropy S at different temperatures for c- Fe_2Hf and h- Fe_2Hf (lower panel), respectively.

Conclusion

In summary, in this work, we theoretically obtain results for structural, elastic, mechanical, electronic, and thermodynamic properties of Fe_2Hf in the cubic and hexagonal solid phases, based on the *ab initio* total energy calculations. The estimated lattice constants are in excellent agreement with the available experimental values. The total energies show that the hexagonal structures are more stable than cubic ones. The DOS at the Fermi level $n(E_F)$ is calculated to be 10.69 states/eV unit cell for cubic and 20.11 eV for hexagonal, indicating the metallic material. Generally speaking, the smaller $n(E_F)$ is, the more stable the compound is. So in agreement with the results obtained from the total energy minimum. The analyses of bulk modulus indicate that all values calculated are exceptionally high, exceeding or matching other hard materials, including boron carbide (B_4C, 200 GPa), silicon carbide (SiC, 248 GPa), sapphire (Al_2O_3, 252 GPa), and cubic boron nitride (*c*-BN, 367 GPa). Unfortunately, for the other computed properties in this work, there are no previous calculations or experimental values to compare with.

Acknowledgments

Taif University Research Supporting Project number (TURSP-2020/66), Taif University, Taif, Saudi Arabia.

References

[1] Koki Ikeda: ferromagnetism in hexagonal and cubic Fe_2Hf compound (1977) 100-101.
[2] S. Kobayashi, K. Kimura, K. Tsuzaki: Intermetallics, 46 (2014) 80-84.
[3] S. Kobayashi, T. Hibaru: ISIJ International, 55 (2015) 293-399.
[4] J. Belosevic-Cavor, V. Koteski, N. Novakovic, G. Concas, F. Congiu, and G. Spano: Euro Phys J B, 50 (2006) 425-430.
[5] M. Takeyama: Materials Science Forum, 3012 (2007) 539-543.
[6] D. Sholl, J.A. Steckel, Density functional theory: a practical introduction, John Wiley & Sons (2011) 17-25.
[7] K.P. Skokov, O. Gutfleisch: Scripta Materialia, 154 (2018) 289-294.
[8] W. Kohn, L.J. Sham: Physical review, 140 (1965) 1133-1138.
[9] J.P. Perdew, K. Burke, M. Ernzerhof: Phy rev letters, 77 (1996) 3865-3871.
[10] O.Y. Vekilova, B. Fayyazi, K.P. Skokov, O. Gutfleisch, C. Echevarria-Bonet, J.M. Barandiaron, A. Kovacs, J. Fischbacher, T. Schrefl, O. Eriksson: Phy Rev B, 99 (2019) 024421-024429.
[11] G. Kresse, D. Joubert: Phy Rev B, 59 (1999) 1758-1763.
[12] D.J. Chadi, M.L. Cohen: Phy Rev B, 8 (1973) 5747-5754.
[13] D. Goll, T. Gross, R. Loeffler, U. Pflanz, T. Vogel, A. Kopp, T Grubesa, G. Schneider Hard: Phy Sta Solidi RRL, 11 (2017) 1700184 (1-4).
[14] A.D. Boese, J.M. Martin, N.C. Handy: J of Chem Phys, 119 (2003) 3005-3014.
[15] A. Tanto, T. Chihi, M.A. Ghebouli, M. Reffas, M. Fatmi, B. Ghebouli: Resu in Phy 9 (2018) 763-770.
[16] F. Weber, L. Pintschovius, W. Reichardt, R. Heid, K.-P.Bohnen, A. Kreyssig, D. eznik, K. Hradil: Phy Rev B, 89 (2014) 10450 (1-13).
[17] M. D. Segall, P.J.D. Lindan, M.J. Probert, C.J. Pickard, P.J. Haspin, S.J. Clark, M.C. Payne: J of Phys Cond Matter, 14 (2002) 2717-2744.
[18] J.P. Perdew, S. Burke, M. Ernzerhof: Phys Rev Letters, 80(4) (1998) 891–891.
[19] L. Fast, J M. Wills, B. Johansson and O. Eriksson: Phys Rev B, 51 (1995) 17431-17438.
[20] M. Born, K. Huang: Dynamical Theory of Crystal Lattices, Clarendon, Oxford, (1956) 120-124.
[21] Q.K. Hu, Q.H. Wu, Y.M. Ma, L.J. Zhang, Z.Y. Liu, J.L. He, H. Sun, H.T. Wang, Y.J. Tian: Phys Rev B, 73 (2006) 214116 (1-5).
[22] P. Ravindran, L. Fast, P. A. Korzhavyi, B. Johansson, J. Wills and O. Eriksson: J of Appl Phys, 84 (1998) 4891-4904.
[23] C.F. Cline, H.L. Dunegan, G.W. Henderson: J of Appl Phys, 38 (1967) 1944-1948.
[24] J. M. Leger, J. Haines, M. Schmidt, J.P. Petitet, A.S. Periera, J.A.H. Da Jornada: Nature, 383 (1996) 401.
[25] S.F. Pugh: Philos Mag, 45 (1954) 823-843.
[26] J. Haines, J.M. leger, G. Bocquillon: Ann Rev of Mater Res, 31 (2001) 1-23.
[27] O.L. Anderson: J Phys Chem of Sol, 24 (7) (1963) 909-917.
[28] R. Hill: Proc. Soc. London A, 65 (1952) 350.
[29] K. B. Panda and K. S. Ravi: Comput Mater Sci, 35 (2006) 134-150.

[30] C. Kittel: Introduction to Solid State Physics, 7th ed. Wiley, New York (1996) 15-21.